Non-dominated Solution Sampling Using Environmental Selection in EMO algorithms

Tomoaki Takagi Keiki Takadama Hiroyuki Sato
Graduate School of Information and Engineering Sciences,
The University of Electro-Communications
1-5-1 Chofugaoka, Chofu, Tokyo, 182-8585 Japan
Email: tomtkg@uec.ac.jp, keiki@inf.uec.ac.jp, h.sato@uec.ac.jp

***Abstract*—This work focuses on the environmental selection methods incorporated in several evolutionary multi-objective optimization (EMO) algorithms for sampling representative non-dominated solutions from a large non-dominated solution set. Evolutionary multi- and many-objective optimization generally provides a large set of non-dominated solutions. They are useful for precisely approximating the Pareto front but harm decision making when selecting one solution among them. Sampling and presenting a representative set of solutions is a promising method for addressing this issue. The selection of a subset of solutions from a large set of solutions is a type of combinatorial optimization problem. Its difficulty is increased by increasing the size of the non-dominated solution set, because the number of selection combinations of the solutions increases exponentially. This work focuses on environmental selection as a reasonable method to sample a solution subset from a large set. We compare 17 environmental selection methods incorporated in EMO algorithms and show that the one-by-one selection or deletion approach is suitable for sampling a representative non-dominated set.**

***Index Terms*—multi- and many-objective optimization, solution sampling, multi-criteria decision making**

I. Introduction

The output of an evolutionary multi-objective optimization (EMO) algorithm is a set of non-dominated solutions, to approximate the Pareto front [1], [2]. To completely utilize the optimization result by collecting all necessary information, an archiving method is generally employed to maintain all the non-dominated solutions obtained during the search. Generally, the number of non-dominated solutions to be archived is significantly high, and its size increases exponentially with an increase in the number of objectives. A large set of non-dominated solutions is useful in approximating the Pareto front. However, a large set of non-dominated solutions negatively affects the decision-making process of selecting one solution among them. Solution sampling to select a representative subset of non-dominated solutions has been studied for decision making involving a large non-dominated set [3].

The sampling of a good solution subset from all non-dominated solutions is a type of combinatorial optimization problem. In previous studies [3], representative solution sampling was performed as a binary-combinatorial optimization problem. For $N_{\mathcal{S}}$ non-dominated solutions, the sampling combination is represented with $N_{\mathcal{S}}$ binary bits. Each bit corresponds to a non-dominated solution. One indicates that the corresponding solution is selected, and zero indicates that the corresponding solution is not selected. However, the total number of sampling combinations increases exponentially on increasing the number of non-dominated solutions; consequently, the difficulty of the sampling optimization also increases. In particular, in the case of many-objective optimization, because we need to consider a large set of non-dominated solutions, a better method for representative sampling solutions is desirable.

In this work, to sample representative non-dominated solutions from a large set of solutions, we focus on *environmental selection* methods, which are built-in mechanisms in EMO algorithms. For example, in the case of NSGA-II [4], the environmental selection selects the elite solution set from all solutions in the population, based on the non-dominated front ranking and the crowding distance. Most of the recent EMO algorithms are elitist ones commonly known as $(\mu+\lambda)$-EAs, and this type of environmental selection is frequently incorporated to maintain good solutions for the Pareto front approximation as the elite set in the population over generations. Therefore, criteria in environmental selections would be useful for the solution sampling from the non-dominated set. In this work, we utilize environmental selection methods to sample a representative set from a large non-dominated solution set instead of not treating the sampling as a combinatorial optimization problem. We compare 17 environmental selection methods incorporated in EMO algorithms on test problems with different Pareto front shapes and two to eight objectives.

II. Non-dominated solution sampling by using environmental selection

In this work, we sample a representative non-dominated solution set $\mathcal{S}'$ ($\subset \mathcal{S}$) using an environmental selection in-

Algorithm 1 Non-dominated solution sampling

Input: $\mathcal{S}$: Non-dominated solutions, $N_{\mathcal{S}'}$: Representative solutions size, Alg : MOEA
Output: $\mathcal{S}'$: Representative solutions ($\mathcal{S}' \subset \mathcal{S}$)

```
1: function SOLUTION SAMPLING(Alg, S, N_S')
2:     S' ← Environmental selection(Alg, S, N_S')
3:     return S'
4: end function
```

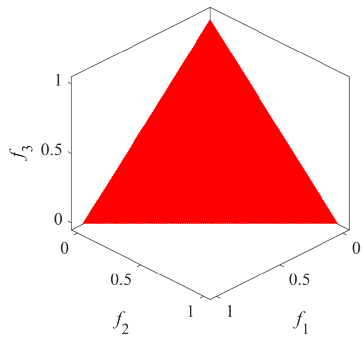

(a) Plane (SMOP1 [8])

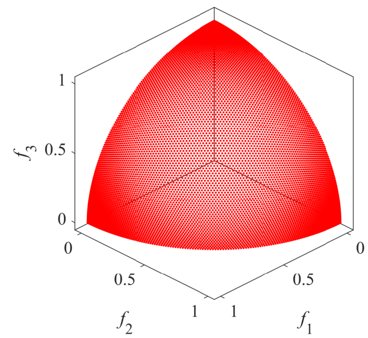

(b) Concave (DTLZ2 [5])

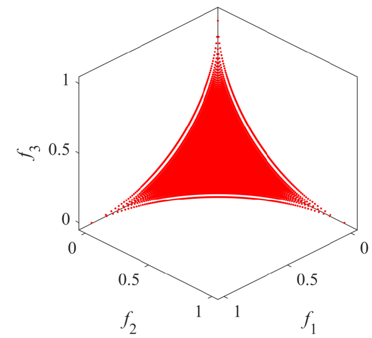

(c) Convex (SMOP4 [8])

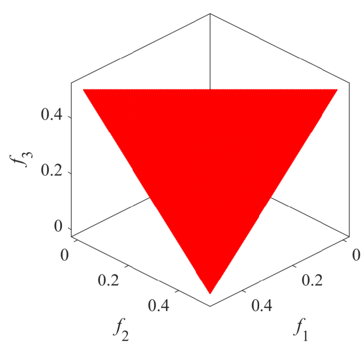

(d) Inverted plane (IDTLZ1 [6])

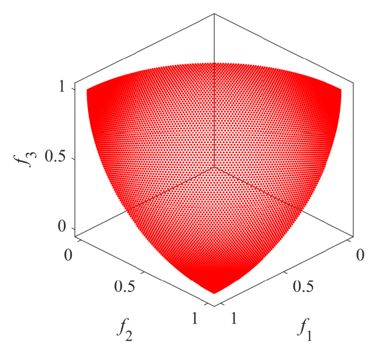

(e) Inverted concave (IDTLZ2 [6])

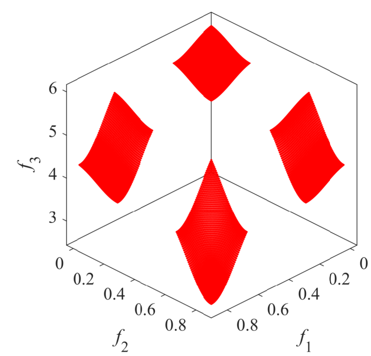

(f) Disconnected (DTLZ7 [5])

Fig. 1: Large non-dominated point sets $\mathcal{S}$ that are supersets of representative sets $\mathcal{S}'$ for three-objective problems

Algorithm 2 Environmental selection of Alg =NSGA-II [4]

Input: $\mathcal{S}$: Non-dominated solutions, $N_{\mathcal{S}'}$: Representative solutions size, Alg : NSGA-II

Output: $\mathcal{S}'$: Representative solutions ($\mathcal{S}' \subset \mathcal{S}$)

function ENVIRONMENTAL SELECTION(NSGA-II, $\mathcal{S}$, $N_{\mathcal{S}'}$)
  $\mathcal{S}' = \emptyset, i = 1$
  $\mathcal{F}_1, \mathcal{F}_2, \ldots \leftarrow$Non-dominated sorting($\mathcal{S}$)
  while $|\mathcal{S}'| + |\mathcal{F}_i| < N_{\mathcal{S}'}$ **do**
    $\mathcal{S}' \leftarrow \mathcal{S}' \cup \mathcal{F}_i$
    $i \leftarrow i + 1$
  end while
  if $|\mathcal{S}'| < N_{\mathcal{S}'}$ **then**
    $\mathcal{F}_i \leftarrow$ Sort by crowding distance($\mathcal{F}_i$)
    $\mathcal{S}' \leftarrow \mathcal{S}' \cup \{\boldsymbol{x}_1, \boldsymbol{x}_2, \ldots, \boldsymbol{x}_{N_{\mathcal{S}'}-|\mathcal{S}'|}\} \subseteq \mathcal{F}_i$
  end if
  return $\mathcal{S}'$
end function

corporated in an EMO algorithm, from a large set of non-dominated solutions $\mathcal{S}$. Algorithm 1 presents the pseudo-code of this process. The inputs are the large set $\mathcal{S}$ involving $N_{\mathcal{S}}$ non-dominated solutions, the size of representative non-dominated solution set $N_{\mathcal{S}'}$ ($\leq N_{\mathcal{S}}$), and a EMO algorithm Alg. Thus, the size of the representative set $N_{\mathcal{S}'}$ is given, and the environmental selection method is specified by the name of the EMO algorithm that incorporates the method.

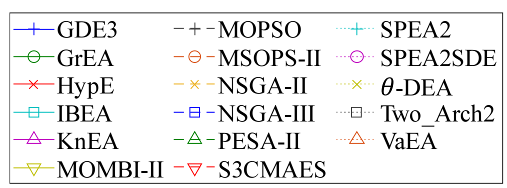

Fig. 2: EMO algorithm and legend list

As an example, Algorithm 2 shows the case where the environmental selection of NSGA-II is specified (Alg = NSGA-II) in Algorithm 1. In the environmental selection of NSGA-II, we select the parent population $\mathcal{S}'$ from the entire population $\mathcal{S}$. The size of the parent population $\mathcal{S}'$ is half of the entire population $\mathcal{S}$, i.e. $N_{\mathcal{S}'} = N_{\mathcal{S}}/2$. However, in this work, the sample size $N_{\mathcal{S}'}$ is specified in Algorithm 1. Thereafter, we select a representative set $\mathcal{S}'$ including the specified number of $N_{\mathcal{S}'}$ solutions from a large non-dominated set $\mathcal{S}$, based on the criterion of NSGA-II.

Similar selection mechanisms are incorporated in several EMO algorithms as the environmental selection. Even if the input non-dominated solution set $\mathcal{S}$ is the same, different environmental selection algorithms select different representative subsets $\mathcal{S}'$. These environmental selections are originally designed to select promising parent solutions $\mathcal{S}'$ from all solutions $\mathcal{S}$ in the entire population, and its ratio is generally

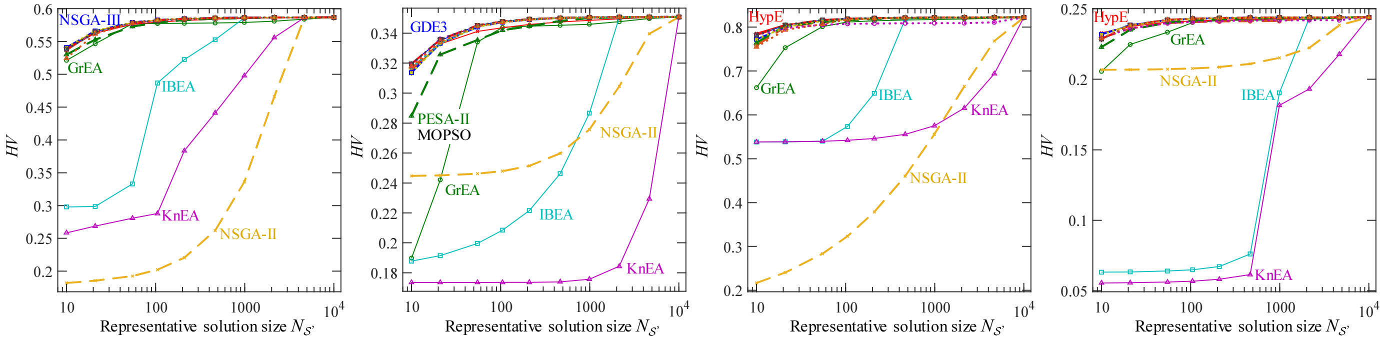

(a) Plane (b) Concave (c) Convex (d) Disconected

Fig. 3: Sampling quality HV of representative set $\mathcal{S}'$ sampled from a large non-dominated set $\mathcal{S}$ when the sample size $N_{\mathcal{S}'}$ varies for two-objective problems ($N_{\mathcal{S}'} = \{10, 21, 55, 105, 210, 465, 990, 2145, 4656, N_{\mathcal{S}}\}$)

one to two between the selected solutions $\mathcal{S}'$ and the all solutions $\mathcal{S}$, i.e. $N_{\mathcal{S}'} : N_{\mathcal{S}} = 1 : 2$. However, in this work, we select a a small number of representative solutions $\mathcal{S}'$ from a large non-dominated solution set $\mathcal{S}$, and the selection ratio of each solution is lower than that for conventional usage.

When the size of the representative set $N_{\mathcal{S}'}$ decreases, the approximation quality of the Pareto front deteriorates. Therefore, the desirable environmental selection method as a non-dominated solution sampler is that which can suppress the deterioration of the approximation quality as much as possible when the sampling size $N_{\mathcal{S}'}$ decreases.

III. Experimental Design

A. Test Problems

In this work, we use six problems with different Pareto front shapes for each of $m = \{2, 3, 4, 8\}$ objective problems, respectively. We focus on DTLZ [5], [6], WFG [7], and SMOP [8] test suites because they have the scalability in the number of objectives and their Pareto fronts are known. As the plane shape, we employ SMOP1, which can also categorize DTLZ1 and SMOP2-3. As a concave shape, we employ DTLZ2, which can also categorize DTLZ3-4, WFG4-9, and SMOP7-8. As a convex shape, we employ SMOP4. SMOP5-6 also has convex Pareto fronts. As an inverted plane shape, we use IDTLZ1. Moreover, as an inverted concave shape, we use IDTLZ2. As a disconnected shape, we use DLTZ7.

For each problem, we generate a large non-dominated point set $\mathcal{S}$. In the case of DTLZ7 that has a disconnected Pareto front, we used $N_{\mathcal{S}} = \{10000, 10000, 10648, 16384\}$ points generated by separating and transforming the uniform grid intersections on $m-1$ dimensional space for $m = \{2, 3, 4, 8\}$ objective problems, respectively. For other problems, we respectively generate $N_{\mathcal{S}} = \{10000, 9870, 9880, 11440\}$ points using the simplex-lattice method on $m = \{2, 3, 4, 8\}$ objective problems, and transform them based on each Pareto front shape. As examples, Fig. 1 depicts the large non-dominated point sets in the $m = 3$ objective space. Although this paper using the above way, there are other alternative ways to generate these non-dominated point sets, i.e., the Riesz s-energy method [9], the Hammersley method [10] and the low-discrepancy sequences method [11].

In this work, we sample a representative set that is the subset of the large non-dominated point set $\mathcal{S}$, using environmental selection.

B. Algorithms

We compare the sampling performance of the representative points of 17 environmental selection methods incorporated in EMO algorithms, including GDE3 [12], GrEA [13], HypE [14], IBEA [15], KnEA [16], MOMBI-II [17], MOPSO [18], MSOPS-II [19], NSGA-II [4], NSGA-III [20], PESA-II [21], S3CMAES [22], SPEA2 [23], SPEA2SDE [24], θ-DEA [25], Two_Arch2 [26], and VAEA [27]. The implementations of PlatEMO [28], which is a program library of EMO algorithms, were utilized in this experiment. For each algorithm, the initial parameter of PlatEMO is employed. Fig. 2 illustrates the algorithm list and the legends used in this paper.

C. Metric

To evaluate the sampling quality of the representative non-dominated points, we measure $Hypervolume$ (HV) [29] of the sampled representative set. The higher the value of HV, the higher is the approximation quality of the Pareto front and the better is the representative set. HV is a volume enclosed by the sampled points and the reference point $\boldsymbol{r}$ in the objective space. The spread of the sampled points in the objective space and the uniformity of sampled points in the objective space affect the value of HV. For each selected point $\boldsymbol{s}' \in \mathcal{S}'$, we normalize its objective values as $s'^{n}_{j} = s'_j / \max_{\boldsymbol{s} \in \mathcal{S}}\{s_j \cdot 1.1\}$ $(j = 1, 2, \ldots, m)$, and subsequently calculate HV of $\mathcal{S}'$ with the reference point $\boldsymbol{r} = \{1.0, 1.0, \ldots, 1.0\}$.

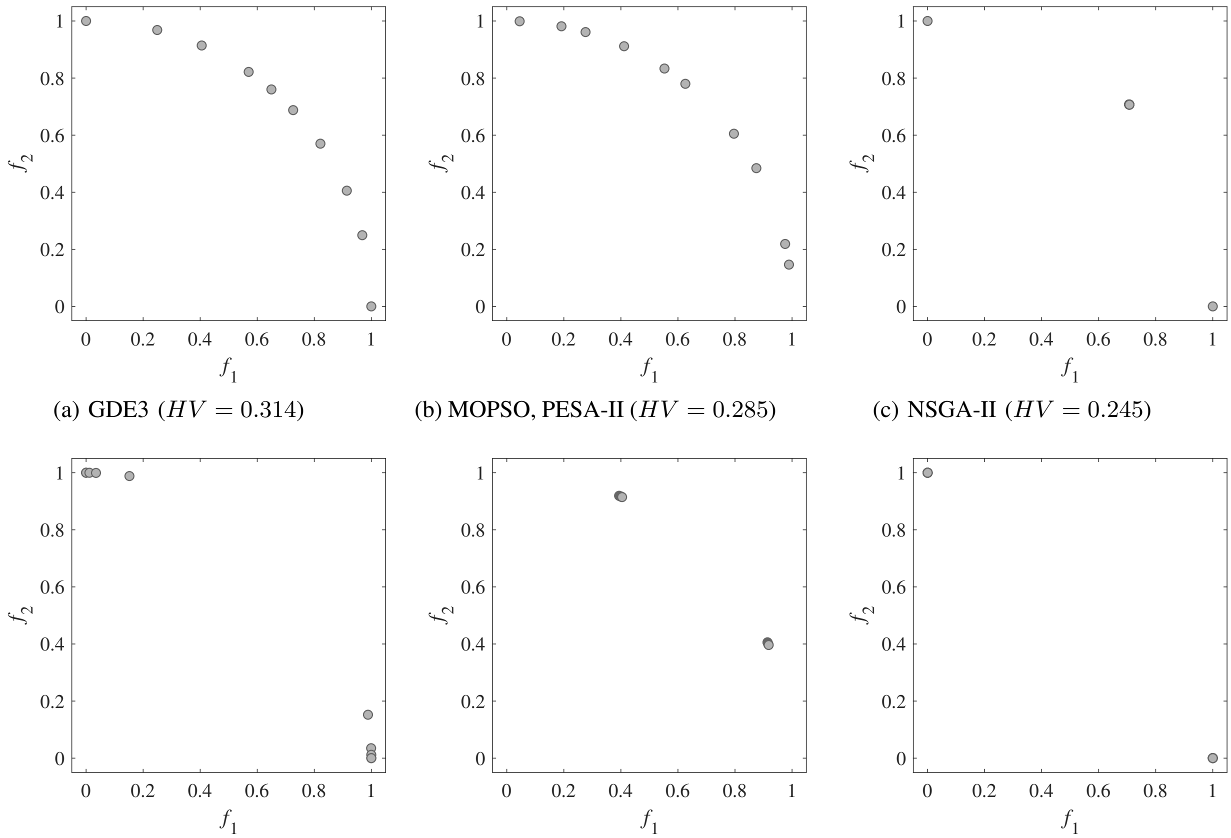

(a) GDE3 ($HV = 0.314$) (b) MOPSO, PESA-II ($HV = 0.285$) (c) NSGA-II ($HV = 0.245$)

(d) GrEA ($HV = 0.190$) (e) IBEA ($HV = 0.188$) (f) KnEA ($HV = 0.174$)

Fig. 4: Sampled representative solution sets with $N_{\mathcal{S}'} = 10$ on a two-objective concave problem

IV. Experimental Results and Discussion

A. Overall Trend

Figs. 3, 5, 8, and 9 show that the results of the sampling quality HV of the representative non-dominated solutions when the sample size $N_{\mathcal{S}'}$ varies for $m = \{2, 3, 4, 8\}$ objective problems, respectively. Each figure describes several names of algorithms that achieved the highest HV with the minimum sample size $N_{\mathcal{S}'}$ or showed a drastic change of HV.

In each figure, the maximum HV can be seen in the case where $N_{\mathcal{S}} = N_{\mathcal{S}'}$ because two sizes of the large non-dominated set $\mathcal{S}$ and the representative set $\mathcal{S}'$ are the same, and no sampling is performed in all the algorithms. As a general tendency, the sampling quality HV decreases by decreasing the size of the representative set $N_{\mathcal{S}'}$. However, we see that the extent of the decrease depends on the algorithm. As a good non-dominated solution sampler, it is desirable to hold a high HV as possible when the sampling size of $N_{\mathcal{S}'}$ decreases.

B. Two Objective Problems

From the results of Fig. 3 for $m = 2$ objective problems, we see that HV values of KnEA and NSGA-II rapidly decrease when the sample sizes are set to $N_{\mathcal{S}'} \leq 2145$ on the problem with the plane Pareto front and $N_{\mathcal{S}'} \leq 4656$ on the problems with the concave and convex Pareto fronts. HV values of IBEA and GrEA also rapidly decrease when $N_{\mathcal{S}'}$ falls below a specific value in all four problems. Thus, the sampling quality HV of each of these algorithms is rapidly deteriorated by decreasing the representative sampling size $N_{\mathcal{S}'}$.

We see that MOMBI-II, NSGA-III, and θ-DEA achieved the highest sampling quality HV with all sizes of $N_{\mathcal{S}'}$ for the plane problem but not the highest for other problems. The reason is that they use decomposition-based environmental selections with uniformly distributed weight vectors or reference lines on the plane surface, which matched with the problem with the plane Pareto front.

GDE3 achieved the highest sampling quality HV at $N_{\mathcal{S}'} = 10$ for the concave problem and the top five HV at any sampling size $N_{\mathcal{S}'}$ for other problems. Both GDE3 and NSGA-II employ crowding distance to rank non-dominated solutions. However, their HV values, especially with a small sampling size $N_{\mathcal{S}'}$, are quite different. NSGA-II calculates the crowding distances for all non-dominated solutions and selects the top $N_{\mathcal{S}'}$ solutions among them in descending order of the crowding distance values at once. Meanwhile, GDE3 calculates the crowding distances for all non-dominated solutions but discards only one worst solution from them. The solution relationships are then changed, and GDE3 re-calculates the crowding distances for the remaining non-dominated solutions

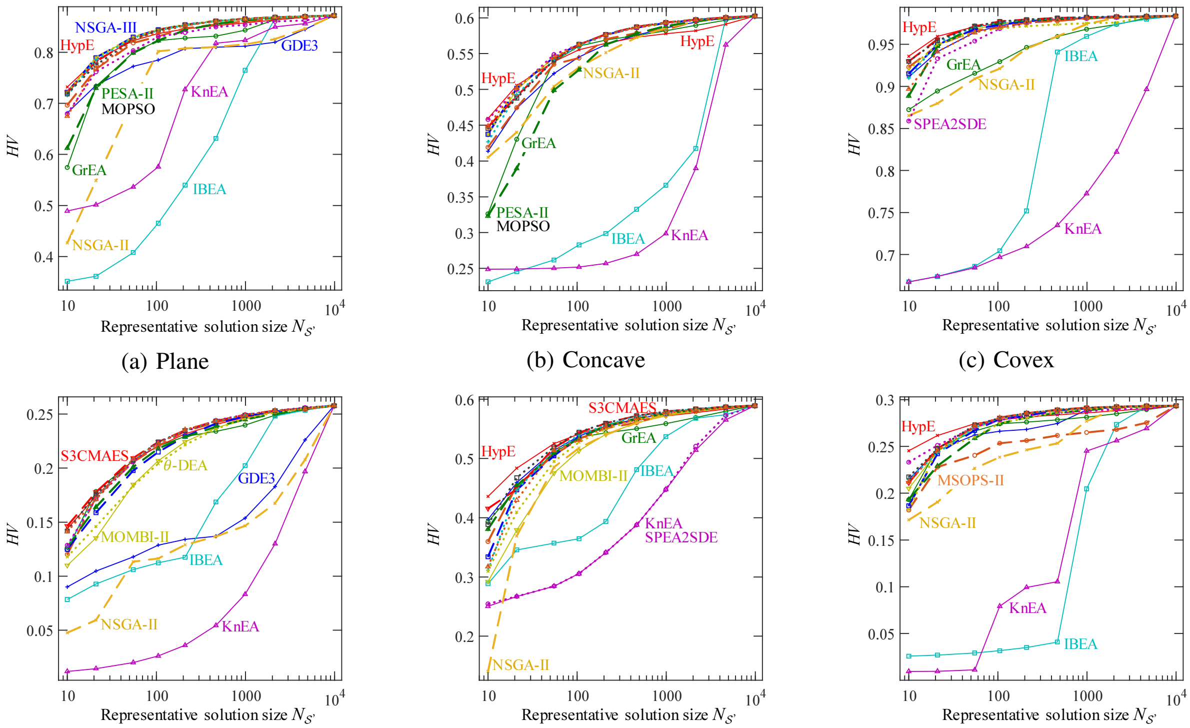

(a) Plane (b) Concave (c) Covex

(d) Inverted plane (e) Inverted concave (f) Disconnected

Fig. 5: The sampling quality HV of the representative set $\mathcal{S}'$ sampled from the large non-dominated set $\mathcal{S}$ when the sample size $N_{\mathcal{S}'}$ varies for three-objective problems ($N_{\mathcal{S}'} = \{10, 21, 55, 105, 210, 465, 990, 2145, 4656, N_{\mathcal{S}}\}$)

and discards the worst solutions again. GDE3 repeats this process until the size of the non-dominated solutions meets the target size of $N_{\mathcal{S}'}$. This result suggests that a one-by-one deletion approach in GDE3 is better than a one-time selection approach in NSGA-II, as solution sampling methods, especially in the case where the sampling size $N_{\mathcal{S}'}$ is smaller than the original size of $N_{\mathcal{S}}$.

HypE achieved the highest HV at $N_{\mathcal{S}'} = 10$ for the convex and disconnected problems. However, in the size range $N_{\mathcal{S}'} \geq 465$, HypE slumps to worst, fourth to sixth place for all problems. HypE calculates the HV contribution of each solution and discards the worst solution with the minimum HV contribution repeatedly. As the initial setting in the PlatEMO program library, HypE uses the reference point $\boldsymbol{r} = \{1.2, 1.2, \dots\}$ in the normalized objective space while the sampling quality HV is calculated with the reference point $\boldsymbol{r} = \{1.1, 1.1, \dots\}$. The difference in the reference points affects the results. HypE is a one-by-one deletion algorithm, such as GDE3. Since the sampling of the representative set is a combinatorial optimization problem, which selects a small subset $\mathcal{S}'$ from a large solution set $\mathcal{S}$. The simple repetition of one-by-one deletion cannot guarantee obtaining a good subset even if the HV contribution is used as the sampling criterion when the deletion size ($N_{\mathcal{S}} - N_{\mathcal{S}'}$) is too large.

S3CMAES achieved the highest HV in many cases of $N_{\mathcal{S}'}$ in the problems except for the plane case. S3CMAES first selects the extreme solutions by using the cosine similarity of each fundamental vector of the objective axes. After that, it repeats one-by-one selection in the order of the $L_{0.5}$ norm from the selected solutions. This result suggests that the one-by-one selection algorithm, such as S3CMAES, is better than the one-by-one deletion algorithm, such as HypE and GDE3, as a representative solution sampler holding the Pareto front approximation quality when the representative set size is small.

Fig. 4 shows characteristic representative sets sampled with $N_{\mathcal{S}'} = 10$ on the concave problem. Each caption describes the algorithm name and its sampling quality HV. When the positions of the sampled solutions are overlapped in the objective space, we cannot see all $N_{\mathcal{S}'} = 10$ points in each figure. We see that the sampling quality HV is high when the sampled solutions are not overlapped and are widely and uniformly distributed in the objective space.

MOPSO and PESA-II employ the same environmental selection algorithm, and their difference is how they generate solutions. In this paper, they do not generate any solutions and are used to sample representative solutions based on their environmental selections. Consequently, their representative sets are the same. MOPSO and PESA-II prepare grids in the objective space and randomly delete one solution from the most crowded grid repeatedly. Because the two algorithms

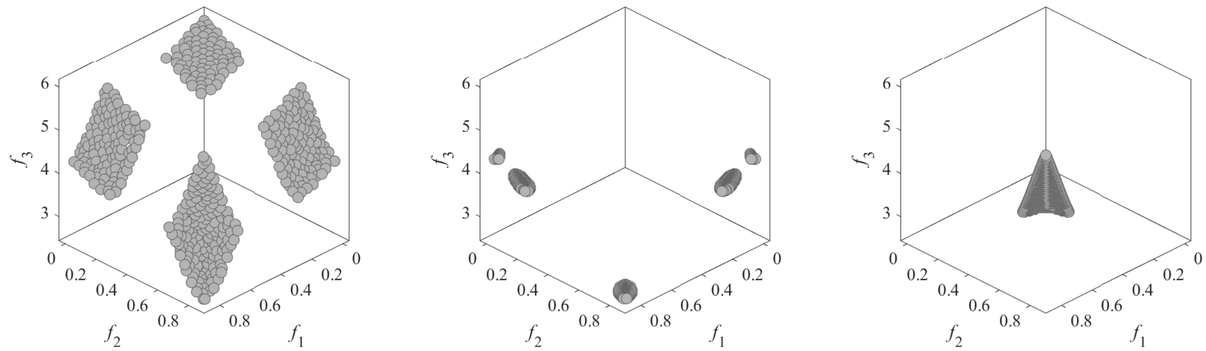

(a) S3CMAES ($HV = 0.289$) (b) KnEA ($HV = 0.105$) (c) IBEA ($HV = 0.041$)

Fig. 6: Sampled representative solution sets with $N_{\mathcal{S}'} = 465$ for three-objective disconnected problems

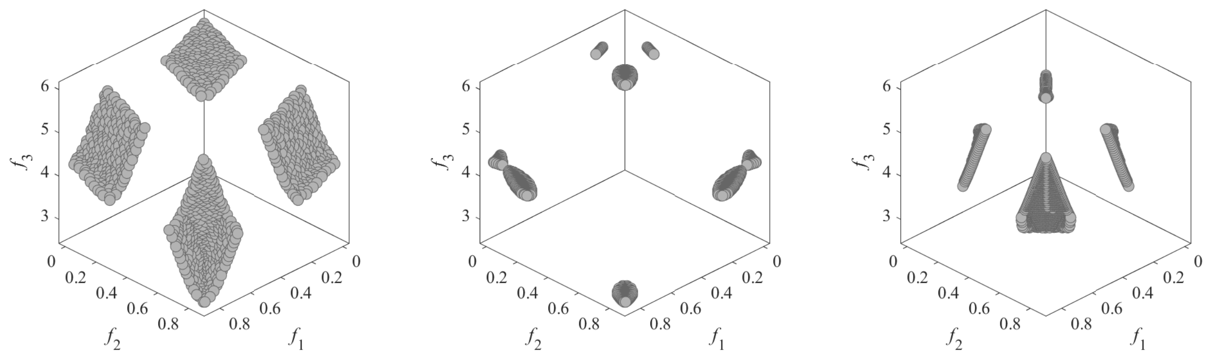

(a) S3CMAES ($HV = 0.291$) (b) KnEA ($HV = 0.245$) (c) IBEA ($HV = 0.205$)

Fig. 7: Sampled representative solution sets with $N_{\mathcal{S}'} = 990$ for three-objective disconnected problem

use grids, they can sample non-overlapped solutions. However, because they randomly choose a solution to be deleted from the most crowded grid, they cannot guarantee the selection of extreme solutions to represent the maximum spread of the Pareto front. Consequently, their sampling quality of HV is not good.

The environmental selection of NSGA-II is a one-time selection. NSGA-II calculates the crowding distances of all solutions and selects $N_{\mathcal{S}'}$ solutions among them in descending order of crowding distances at once. In this paper, as a large non-dominated solution set $\mathcal{S}$, we generate several uniformly distributed points on a plane and transform the plane based on the shape of the Pareto front. In the case of the concave Pareto front, the points are distributed densely around the edge of the Pareto front and sparsely around the center of the Pareto front due to the transformation of the point distribution fit to the concave Pareto front. Consequently, points around the center of the Pareto front have a long crowding distance and are selected next to the extreme solutions having the infinite crowding distances. As a result, the biased solutions are sampled by NSGA-II shown in Fig. 4.

GrEA sets grids in the objective space and calculates three grid-based fitness values for each solution. Three fitness values are prioritized to compare the solutions, and the highest one is the grid rank GR. GR is the Manhattan distance between a solution and the origin on the grid coordinate, and a solution with a small GR is selected with high priority. In the case of the concave problem, solutions around the extreme area tend to have a smaller GR than others and are selected with high priority. As a result, solutions sampled by GrEA are distributed in extreme areas in the objective space.

IBEA calculates the fitness values for all solutions repeatedly and deletes the worst solution until the remaining solution set is shrunk to the target size $N_{\mathcal{S}'}$. Thus, IBEA is a one-by-one deletion algorithm such as HypE and GDE3. However, as shown in Fig. 4, the sampled solutions were distributed in two specific areas. IBEA needs the setting of the parameter κ, and $\kappa = 0.05$ is used in this work as the common setting. Because κ affects the fitness value calculation, a more appropriate κ for this kind of sampling task may exist.

KnEA performs a one-time selection as with NSGA-II. KnEA first assesses each solution in a large set. KnEA then selects $N_{\mathcal{S}'}$ solutions based on the assessment at once. As shown in Fig. 4, many solutions in two extreme areas are highly ranked and selected. As a result, KnEA can not sample solutions between them.

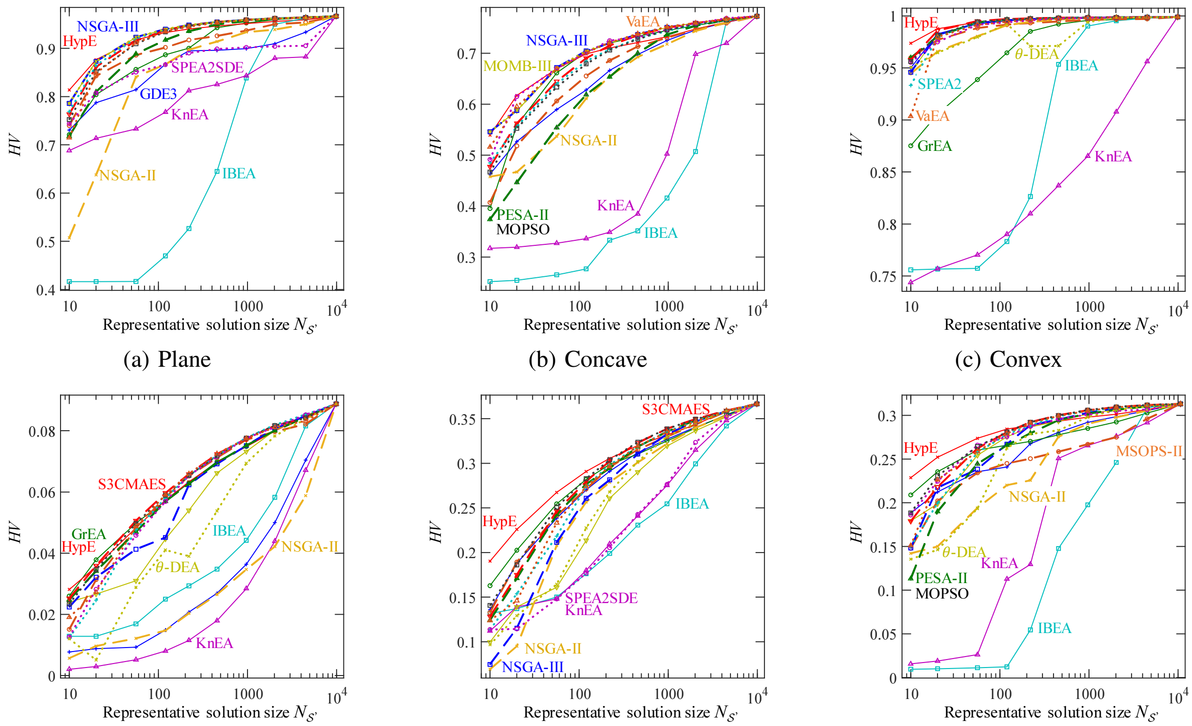

(a) Plane (b) Concave (c) Convex

(d) Inverted plane (e) Inverted concave (f) Disconnected

Fig. 8: The sampling quality HV of the representative set $\mathcal{S}'$ sampled from a large non-dominated set $\mathcal{S}$ when the sample size $N_{\mathcal{S}'}$ varies for four-objective problems ($N_{\mathcal{S}'} = \{10, 20, 56, 120, 220, 455, 969, 2024, 4495, N_{\mathcal{S}}\}$)

C. Three Objective Problems

Fig. 5 shows results for $m = 3$ objective problems. From these results, we see that the sampling quality of HV values of IBEA, KnEA, NSGA-II, and GrEA are relatively lower than others, especially when the sampling size $N_{\mathcal{S}'}$ is small. This is a similar tendency to the results for $m = 2$ objective problems shown in Fig. 3.

SPEA2SDE is a variant of SPEA2, and it calculates the shift-distance between two solutions in the objective space and discards the worst solution with the shortest distance from the population repeatedly. SPEA2SDE achieved the second-best HV at $N_{\mathcal{S}'} = 10$ for the concave and the disconnected problems. However, SPEA2SDE shows the third-worst HV at $N_{\mathcal{S}'} = 10$ for the convex and inverted concave problems, and the worst HV at many sampling sizes $N_{\mathcal{S}'}$ for the inverted concave problem. Thus, the sampling quality of SPEA2SDE depends on the problem characteristics.

The sampling quality HV of the decomposition-based algorithms, such as MOMBI-II and θ-DEA, is deteriorated for the inverted problems. These algorithms use a predefined set of weight vectors, and they are generated based on the simplex-lattice design, assuming a regular triangle shape. Because the inverted problems have inverted triangle Pareto fronts, the weight vector distribution does not match their Pareto fronts, and the HV values become low in these problems. These algorithms select many solutions around the edge of the Pareto front and fewer solutions around the center of the Pareto front.

The algorithm ranks of GDE3 for $m = 3$ objective problems are lower than that for $m = 2$ objective problems. GDE3 employs the crowding distance to rank the non-dominated solutions. Because the crowding distance works well with a two-dimensional space but not a three- or higher-dimensional space, the sampling quality HV is deteriorated for $m = 3$ objective problems.

HypE achieved the highest HV at $N_{\mathcal{S}'} = 10$ for five out of six problems. However, HypE with a large $N_{\mathcal{S}'}$ shows a lower HV than others. This is a similar tendency shown in the $m = 2$ objective problems.

From these results, we see that the decomposition-based algorithms achieved better sampling quality for the plane problem, and S3CMAES achieved better quality for other problems.

Fig. 6 and Fig. 7 respectively show characteristic representative sets with $N_{\mathcal{S}'} = \{465, 990\}$ for the disconnected problem. From the results, we see that $N_{\mathcal{S}'} = 465$ solutions sampled by S3CMAES fully covered the four different parts of the Pareto front. However, KnEA and IBEA with $N_{\mathcal{S}'} = 465$ solutions cannot fully cover the four parts. When we increase the sampling size to $N_{\mathcal{S}'} = 990$, although KnEA and IBEA select solutions for the four different parts, the entire picture

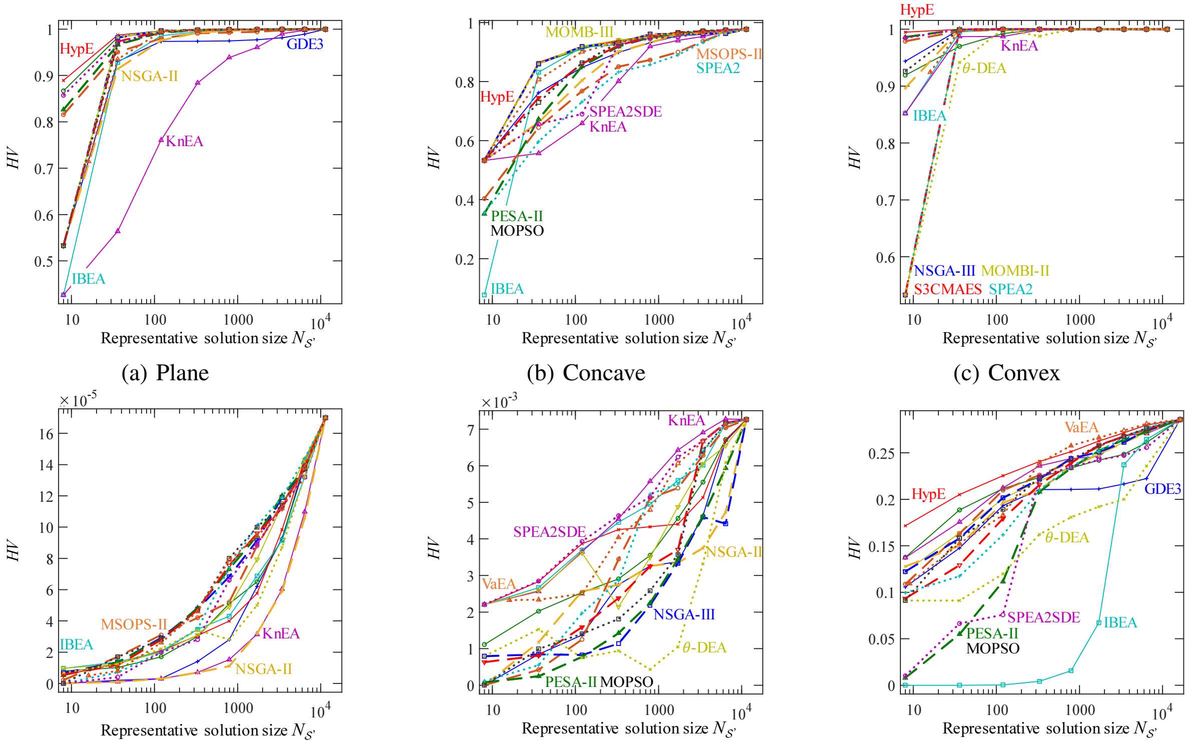

(a) Plane (b) Concave (c) Convex

(d) Inverted plane (e) Inverted concave (f) Disconnected

Fig. 9: The sampling quality HV of the representative set $\mathcal{S}'$ sampled from a large non-dominated set $\mathcal{S}$ when the sample size $N_{\mathcal{S}'}$ varies for eight-objective problems ($N_{\mathcal{S}'} = \{8, 36, 120, 330, 792, 1716, 3432, 6435, N_{\mathcal{S}}\}$)

of the Pareto front cannot be seen.

D. Four Objective Problems

Fig. 8 shows the sampling performance of HV for the $m = 4$ objective problems. The results of GDE3, HypE, IBEA, KnEA, NSGA-II, and SPEA2SDE show a similar tendency shown in $m = \{2, 3\}$ objectives.

For the convex and the inverted plane problem, the sampling quality HV of θ-DEA with $N_{\mathcal{S}'} = 120$ is higher than that with $N_{\mathcal{S}'} = 220$. θ-DEA uses the predefined set of weight vectors. The result shows that the weight vector distribution has an impact on the sampling performance, and even if the sampling size and the weight size, are small, solutions with a high approximation quality can be obtained.

The algorithm ranks of GrEA for the inverted and disconnected problems are higher than those for the plane and the convex problems. This result reveals that GrEA achieves a robust sampling quality for the problems having irregular shapes of the Pareto fronts.

E. Eight Objective Problems

Fig. 9 shows the result of the sampling quality for $m = 8$ objective problems. From the result, we see that the relationship between the sampling size $N_{\mathcal{S}'}$ and the sampling quality HV changes drastically when the Pareto front shape changes. For the plane and convex problem, HV rapidly decreases from $N_{\mathcal{S}'} = 36$ to $N_{\mathcal{S}'} = 8$. These values show the minimum sampling size to show a rough picture of the high-dimensional Pareto front.

V. Conclusions

In this work, to sample representative solutions from a large set of non-dominated solutions, we focus on utilizing environmental selection mechanisms incorporated in several EMO algorithms as a representative solution sampler. These environmental selections are originally designed to select promising parent solutions from all solutions in the population, and its ratio is typically one to two between the selected solutions and all solutions. Additionally, in this work, we select a small number of representative solutions from a large non-dominated solution set, and the selection ratio of each solution was lower than that for conventional use. We compared 17 types of environmental selections on problems with different Pareto front shapes and objectives, and the following findings were obtained:

1) One-by-one selection or deletion is better than one-time selection for representative solution sampling.
2) For two to four objective problems, HypE is a promising method if the representative solution size $N_{\mathcal{S}'}$ is less

than approximately 20; otherwise, S3CMAES is the promising method.

3) For problems with a plane Pareto front, decomposition-based methods prove to be promising.
4) As the number of objectives increases, it becomes difficult to find an appropriate environmental selection.

As future research, we are designing a representative solution sampler by modifying a one-time selection method into a one-by-one selection/deletion scheme, by repeating the one-time selection to delete one solution. Furthermore, we also plan to address interactive representative solution sampling for interactive decision making.

REFERENCES

[1] K. Deb, *Multi-Objective Optimization using Evolutionary Algorithms*, John Wiley & Sons, 2001.

[2] C. A. C. Coello and D. A. V. Veldhuizen, and G. B. Lamont, *Evolutionary Algorithms for Solving Multi-Objective Problems*, Boston, Kluwer Academic Publishers, 2002.

[3] H. Ishibuchi, Y. Sakane, N. Tsukamoto, and Y. Nojima, "Selecting a small number of representative non-dominated solutions by a hypervolume-based solution selection approach," *Proc. of IEEE International Conference on Fuzzy Systems (FUZZ 2009)*, pp. 1609–1614, 2009.

[4] K. Deb, A. Pratap, S. Agarwal, and T. Meyarivan, "A fast elitist multi-objective genetic algorithm: NSGA-II," *IEEE Trans. on Evolutionary Computation*, Vol. 6, pp. 182–197, 2002.

[5] K. Deb, L. Thiele, M. Laumanns and E. Zitzler, "Scalable multi-objective optimization test problems," *Proc. of IEEE Congress on Evolutionary Computation (CEC 2002)*, pp. 825–830, 2002.

[6] H. Jain, K. Deb, "An evolutionary many-objective optimization algorithm using reference-point based nondominated sorting approach, Part II: Handling constraints and extending to an adaptive approach," *IEEE Trans. on Evolutionary Computation*, Vol. 18, No. 4, pp. 602–622, 2014.

[7] S. Huband, P. Hingston, L. Barone, and L. While, "A review of multi-objective test problems and a scalable test problem toolkit," *IEEE Trans. on Evolutionary Computation*, Vol. 10, No. 5, pp. 477–506, 2006.

[8] Y. Tian, X. Zhang, C. Wang, and Y. Jin, "An evolutionary algorithm for large-scale sparse multi-objective optimization problems," *IEEE Trans. on Evolutionary Computation*, 2019.

[9] D. P. Hardin and E. B. Saff, "Minimal Riesz energy point configurations for rectifiable d-dimensional manifolds," *Advances in Mathematics*, Vol. 193, No. 1, pp 174–204, 2005.

[10] J. A. M. Berenguer and C. A. C. Coello, "Evolutionary many-objective optimization based on kuhn-munkres' algorithm," *Proc. of International Conference on Evolutionary Multi-Criterion Optimization (EMO 2015)*, pp. 3–17, Springer, Cham, 2015.

[11] S. Z. Martínez, H. E. Aguirre, K. Tanaka, and C. A. C. Coello, "On the low-discrepancy sequences and their use in MOEA/D for high-dimensional objective spaces," *Proc. of IEEE Congress on Evolutionary Computation (CEC2015)*, pp. 2835–2842, 2015.

[12] S. Kukkonen and J. Lampinen, "GDE3: The third evolution step of generalized differential evolution," *Proc. of IEEE Congress on Evolutionary Computation (CEC 2005)*, pp. 443–450, 2005.

[13] S. Yang, M. Li, X. Liu, and J. Zheng, "A grid-based evolutionary algorithm for many-objective optimization," *IEEE Trans. on Evolutionary Computation*, Vol. 17, No. 5, pp. 721–736, 2013.

[14] J. Bader and E. Zitzler, "HypE: An algorithm for fast hypervolume-based many-objective optimization," *IEEE Trans. on Evolutionary Computation*, Vol. 19, No. 1, pp. 45–76, 2011.

[15] E. Zitzler and S. Kunzli, "Indicator-based selection in multiobjective search," *Proc. of International Conference on Parallel Problem Solving from Nature (PPSN 2004)*, pp. 832–842, Springer, Heidelberg, 2004.

[16] X. Zhang, Y. Tian, and Y. Jin, "A knee point-driven evolutionary algorithm for many-objective optimizatio," *IEEE Trans. on Evolutionary Computation*, Vol. 19, No. 6, pp. 761–776, 2015.

[17] R. H. Gómez and C. A. C. Coello, "Improved metaheuristic based on the R2 indicator for many-objective optimization," *Proc. of Annual Conference on Genetic and Evolutionary Computation (GECCO 2015)*, pp. 679–686, 2015.

[18] C. A. C. Coello and M. S. Lechuga, "MOPSO: A proposal for multiple objective particle swarm optimization," *Proc. of IEEE Congress on Evolutionary Computation (CEC 2002)*, pp. 1051–1056, 2002.

[19] E. J. Hughes, "MSOPS-II: A general-purpose many-objective optimiser," *Proc. of IEEE Congress on Evolutionary Computation (CEC 2007)*, pp. 3944–3951, 2007.

[20] K. Deb, and H. Jain, "An evolutionary many-objective optimization algorithm using reference-point based nondominated sorting approach, Part I: Solving problems with box constraints," *IEEE Trans. on Evolutionary Computation*, Vol. 18, No. 4, pp. 577–601, 2014.

[21] D. W. Corne, N. R. Jerram, J. D. Knowles, and M. J. Oates, "PESA-II: Region-based selection in evolutionary multiobjective optimization," *Proc. of Annual Conference on Genetic and Evolutionary Computation (GECCO 2001)*, pp. 283–290, 2001.

[22] H. Chen, R. Cheng, J. Wen, H. Li, and J. Weng, "Solving large-scale many-objective optimization problems by covariance matrix adaptation evolution strategy with scalable small subpopulations," *Information Sciences*, Vol. 509, pp. 457–469, 2018.

[23] E. Zitzler, M. Laumanns, and L. Thiele, "SPEA2: Improving the strength Pareto evolutionary algorithm," *TIK-report*, Vol. 103, 2001.

[24] M. Li, S. Yang, and X. Liu, "Shift-based density estimation for Pareto-based algorithms in many-objective optimization," *IEEE Trans. on Evolutionary Computation*, Vol. 18, No. 3, pp. 348–365, 2014.

[25] Y. Yuan, H. Xu, B. Wang, and X. Yao, "A new dominance relation-based evolutionary algorithm for many-objective optimization," *IEEE Trans. on Evolutionary Computation*, Vol. 20, No.1, pp. 16–37, 2016.

[26] H. Wang, L. Jiao, and X. Yao, "Two_Arch2: An improved two-archive algorithm for many-objective optimization," *IEEE Trans. on Evolutionary Computation*, Vol. 19, No. 4 pp. 524–541, 2015.

[27] Y. Xiang, Y. Zhou, M. Li, and Z. Chen, "A vector angle-based evolutionary algorithm for unconstrained many-objective optimization," *IEEE Trans. on Evolutionary Computation*, Vol. 21, No. 1, pp. 131–152, 2017.

[28] Y. Tian, R. Cheng, X. Zhang, and Y. Jin, "PlatEMO: A MATLAB platform for evolutionary multi-objective optimization [educational forum], *IEEE Computational Intelligence Magazine*, Vol. 12, No. 4, pp. 73–87, 2017.

[29] E. Zitzler, *Evolutionary Algorithms for Multiobjective Optimization: Methods and Applications*, PhD thesis, Swiss Federal Institute of Technology, Zurich, 1999.